International Proceeding
Universitas Tulungagung
2025

ANALYSIS ON AEROELASTICITY AND THERMAL LOADING OF A ROCKET FIN: EFFECTS OF THICKNESS REDUCTION AND BRACKET SUPPORT

Firza Fadlan Ekadj[1], Wahyu Nirbito[2]*, Fadilah Hasim[3], Matza Gusto Andika[4]
[1,2]Universitas Indonesia, Indonesia
[3,4]Badan Riset dan Inovasi Nasional, Indonesia
*Corresponding author: bito@eng.ui.ac.id

Abstract

Rocket fins serve to stabilize a rocket during flight but are prone to flutter, necessitating an aeroelastic analysis to determine their susceptibility. This study presents the effect of bracket models' inclusion in a computational aeroelastic analysis on a supersonic fin, and the effect on thermal loading of a supersonic fin resulting from a reduction of fin thickness from 25 mm to 12 mm. Using finite element models and the P–K method, flutter onsets were identified at Mach 11.0 for the bracket-free fin and Mach 10.6 for the fin with brackets, both values substantially exceeding the required design criterion of Mach 3.99. These results show that the inclusion of bracket models has only a marginal effect on aeroelastic behavior, while the thinner fin maintains structural stability. Thermal analyses further revealed that the 12-mm fin experiences lower surface temperatures than the 25-mm fin, possibly due to its smaller leading edge's inclination angle. Future investigations should expand on structural loading scenarios to ensure comprehensive design validation.

Keywords: *aeroelasticity, fin, thermal analysis, bracket, rocket*

INTRODUCTION

Rocket fins are structural extensions mounted on the rocket body that serve a crucial function in stabilizing the spacecraft during flight, helping it maintain its intended path and orientation (Salleh et al., 2024; Ujjin, 2021). However, a fin is susceptible to flutter, a phenomenon of severe dynamic instabilities that can induce self-sustained oscillations and may lead to failure (Martins et al., 2022). To determine the susceptibility of the fin to flutter, an aeroelastic analysis must be conducted, which could be done computationally.

To attach the fins to the body of the rocket, brackets can serve as joints and be placed at the root of the fins (Simmons et al., 2009). The addition of brackets would increase the complexity of the structural model and the aerodynamic model of the aeroelastic analysis. A comparison study of aeroelastic analyses with brackets included and excluded is needed to determine whether brackets are necessary in an aeroelastic analysis. Bolt/nut systems are used to fasten the brackets to the fin. The importance of these fasteners is critical since the omission of them could lead to catastrophic failure (Crotty, 1998). Adequate models for representing

these fasteners are needed in order for the computational analyses using brackets to be sufficient.

In multidisciplinary work on a rocket redesign, a change to a rocket's attribute may lead to a safety investigation of the changed attribute. To achieve a larger flight range, a rocket could have a lower mass by redesigning its structure. A straightforward method of reducing the mass of its fins is by reducing the thickness. However, in a supersonic rocket, a fin can be subjected to structural damage due to the aerodynamic heating (Ognjanović et al., 2017). Therefore, a thermal analysis on a reduced-thickness fin is needed to see whether the modification is advantageous in terms of thermal loading.

The novelty of this paper lies in the comparative study of aeroelastic analyses of a fin with and without bracket models. In the aspect of thermal loading, aerodynamic heating on high-speed surfaces has been studied before (Zhiqiang et al., 2018; Chen et al., 2018; Mazzoni et al., 2005; Yang et al., 2021; Wang et al., 2023; Chen et al, 2025; Kuzenov et al., 2022). This study, however, consists of a comparative analysis due to a change in fin thicknesses.

The results show that the flutter onset for the 12-mm fin occurred at Mach 11.0 without brackets and Mach 11.3 with brackets. Both are significantly higher than the design requirement of Mach 3.99. This finding indicates that the inclusion of brackets has only a marginal impact on flutter behavior and that the thinner fin maintains sufficient aeroelastic stability. Thermal analyses further reveal that the 12-mm fin generally has a lower surface temperature than that of the original 25-mm fin, indicating lower aerodynamic heating.

LITERATURE REVIEW

The cause of an aircraft accident has been reported by a technical bulletin (Crotty, 1998). It has been identified that the reason was the omission of fasteners. This led to a structural failure in the brackets connecting the wing-support structure to the ribs of the left wing. The topic holds particular relevance to the present study, which involves the use of bracket fasteners. Recognizing the accident is significant, as it exemplifies the potential for catastrophic failure resulting from noncompliance with safety requirements. A computational aeroelastic analysis has been made on the 12-mm-thick fin in this study without fastener models (Ekadj et al., 2025). In the practical application of flight test, the fasteners are present.

The computational tool used for modal analyses was used by Syamsuar et al. in their study (Syamsuar et al., 2018). The subject of their study was a lifting surface; therefore, it has a similarity with the subject of this study. The topic of discussion of this study, following modal analyses, is aeroelastic analyses. Ju and Qin highlighted the growing dominance of the P–K method within the field of aeroelastic engineering (Ju & Qin, 2009). In view of its prevalent use, the method is utilized in the present study for aeroelastic analyses.

In the discussion of thermal loading on fins, this study refers to studies that consist of supersonic flow theory to give a possible explanation for the analyses' results. Several studies have been conducted on supersonic flow over a wedge (Wolff et al., 2024; Voklov, 2022; Khan et al., 2019). The cited studies are relevant, as the leading-edge geometry of the supersonic fins analyzed in the present work closely corresponds to that of a wedge.

RESEARCH METHOD

A supersonic rocket has been flight-tested using fins with a thickness of 25 mm. Figure 1 shows a fin with a thickness of 25 mm used in this study. The rocket was predicted to reach a maximum flight speed of Mach 3.27, and the flight test did not indicate a structural failure on the fins. A new fin design with a reduced thickness of 12 mm has been made as a possible design replacement in order for the rocket to reach a larger range of flight. An aeroelastic analysis has been conducted for the new design, and it resulted in a flutter speed of Mach 11, considerably higher than the predicted maximum flight speed of the flight-tested rocket. This design has a mass 51.5% lower than the original design.

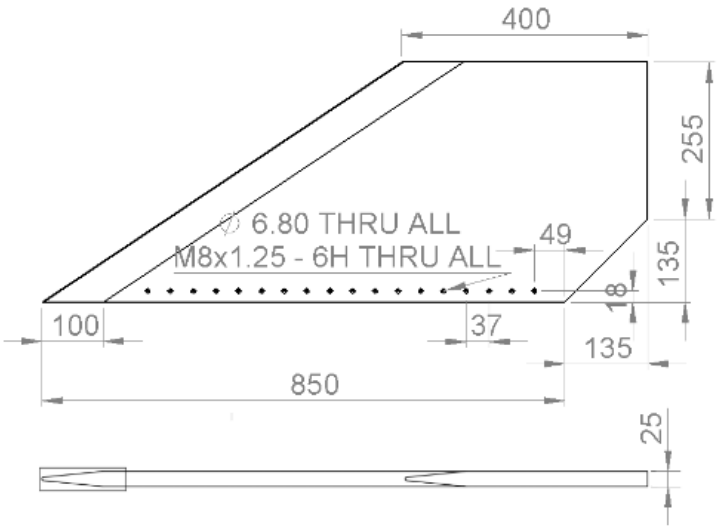

Figure 1. A 25-mm-thick supersonic fin

The material used for the supersonic fins in this study is the same as the fin material used for the flight-tested rocket, i.e., Aluminium alloy 7075. Table 1 shows the properties used for the analyses.

Table 1. Aluminium alloy 7075 properties used for the analyses in this study

Property	Value
Poisson Ratio	0.33
Density (kg/m^3)	2810
Young Modulus (GPa)	70.8

Source: Ekadj et al., in press

The computational modal analysis used NASTRAN's Sol 103, which is capable of solving the following eigenvalue equation (Syamsuar et al., 2018):

$$([K] - \omega_i{}^2[M])\{\phi\}_i = \{0\}$$

where $[K]$ is the generalized stiffness matrix, ω_i is the natural frequency, $[M]$ is the generalized mass matrix, and $\{\phi\}_i$ is the modal eigenvector. The fin is fastened to the brackets by bolt/nut systems, which can be removed without damaging the assembly. The models of the fin and one

of the brackets used for this study are shown in Figure 2. To represent the fasteners in the overall structural model for analysis, the authors used line elements with a property of a spring. Each end of the elements is connected to the structural models of the fin and brackets using Multiple-Point Constraints or MPC, as shown in Figure 3. For the value of the spring constant, a reference that has a considerable similarity in the joint system is used to test its suitability. A sufficient value is determined when the computational analysis result is close to the experimental result.

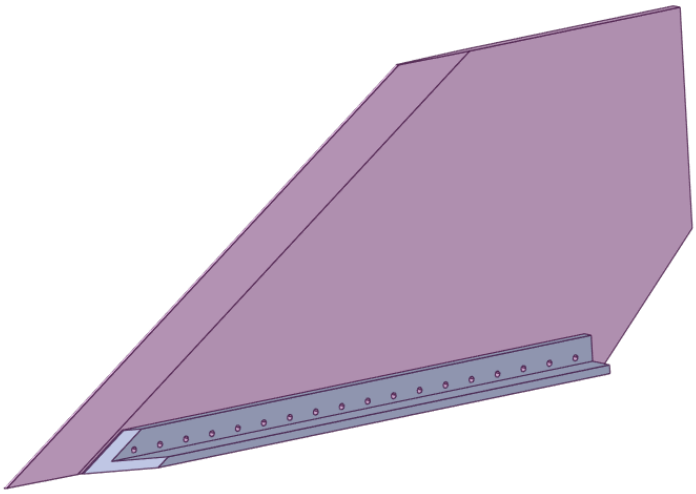

Figure 2. A fin with a bracket

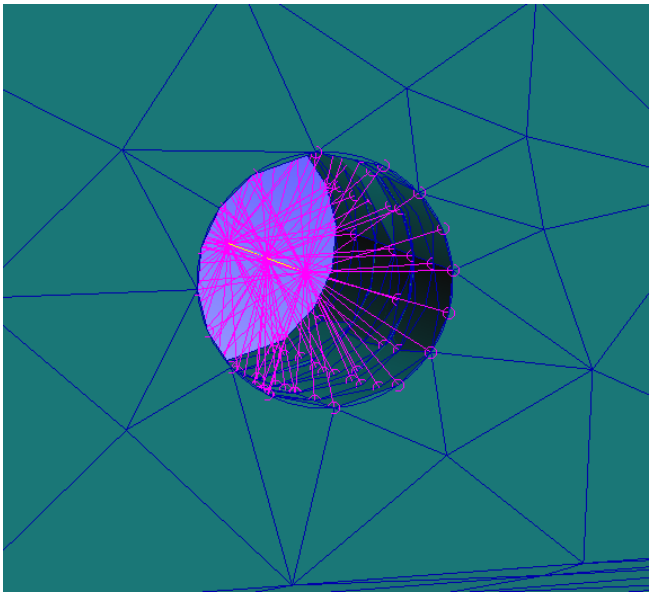

Figure 3. Line elements and MPC representing a fastener

P-K method has emerged as the most widely adopted approach in aeroelastic engineering; therefore, it is used for computational flutter analyses in this study (Ju & Qin, 2009). The flutter equation associated with the p–k method can be expressed as (Rodden, 1979):

$$\left[[M_{hh}]p^2 + \left([B_{hh}] - \frac{1}{4}\rho\bar{c}V[Q^I_{hh}(k)]/k\right)p + \left([K_{hh}] - \frac{1}{2}\rho V^2[Q^R_{hh}(k)]\right)\right]\{u_h\} = 0$$

where M_{hh} is the generalized modal mass, B_{hh} is the damping matrix, K_{hh} is the stiffness matrix, Q^I_{hh} is the real part of the aerodynamic generalized coefficient matrix, Q^I_{hh} is the imaginary part of the aerodynamic generalized coefficient matrix, ρ is the air density, $\bar{c}$ is the reference chord, k is the reduced frequency, V is velocity, and p is a parameter defined by

$$p^2 = -\frac{V^2}{1 + ig}$$

where g is the artificial structural damping coefficient.

For computational modal and aeroelastic analyses purposes, any design is represented using a finite element model (Cavallo et al., 2017; Bramsiepe et al., 2020). To facilitate the management of aeroelastic models, including highly complex ones, Patran features a dedicated tool called Flightloads (Cestino et al., 2019). This tool enables the creation of flat plate aeromodelling (Hexagon AB, 2021). The computational aeroelastic analyses were performed using the ZONA51 code, which is based on Jones' supersonic theory (Jones, 1948; Chen, P.-C., & Liu, 1985).

The thermal analyses are conducted using the fluid-structure interaction method, with thermal properties serving as transfer data between the solid and fluid regions. Coupling participants of ANSYS used for the simulations were Fluid Flow (Fluent) and Transient Thermal, while the System Coupling Service managed the execution of the analyses (ANSYS, Inc., 2018). The input for the simulations is based on a flight condition of a flight speed of Mach 3.27 and sea-level air density.

RESULT AND DISCUSSION

Table 2 shows the computational modal analysis result of the supersonic 12 mm thick fin without bracket models, along with the comparison to the experimental result.

Table 2. Comparison of the natural frequencies of the 12 mm thick fin between the computational result without bracket models and the experimental result

No.	Experimental frequency	Computational frequency	Percent error	Vibration mode
1	66.3 Hz	67.4 Hz	1.7	1st bending
2	143.8 Hz	141.9 Hz	1.3	1st torsion
3	293.1 Hz	289.8 Hz	1.1	2nd torsion
4	381.3 Hz	383.1 Hz	0.5	2nd bending
5	524.4 Hz	523.3 Hz	0.2	3rd bending

Source: Ekadj et al., in press

Aeroelastic analysis using this model resulted in a flutter speed of Mach 11 (Ekadj et al., in press). The predicted flutter Mach number is approximately 2.8 times greater than the design requirement of Mach 3.99, which is obtained by applying a safety factor of 1.22 to the maximum operational speed of Mach 3.27.

Table 3 shows the computational modal analysis results of the supersonic 12 mm thick fin with bracket models using a spring constant chosen from a reference, i.e., 1.15×10^8 N/m^2 (Wemming et al., 2023). The reference is selected due to the similarity in the joint system, which fastens three specimens under the same bolted joint. The computational result is shown to have close agreement with the experimental result. Using the value of the spring constant, the models used to represent the fasteners have been made sufficient to be used for further analyses.

Table 3. Comparison of the natural frequencies of the 12 mm thick fin between the computational result with bracket models and the experimental result

No.	Experimental frequency	Computational frequency	Percent error
1	66.3 Hz	66.7 Hz	0.5
2	143.8 Hz	140.7 Hz	2.1
3	293.1 Hz	287.6 Hz	1.9
4	381.3 Hz	379.1 Hz	0.6
5	524.4 Hz	520.7 Hz	0.7

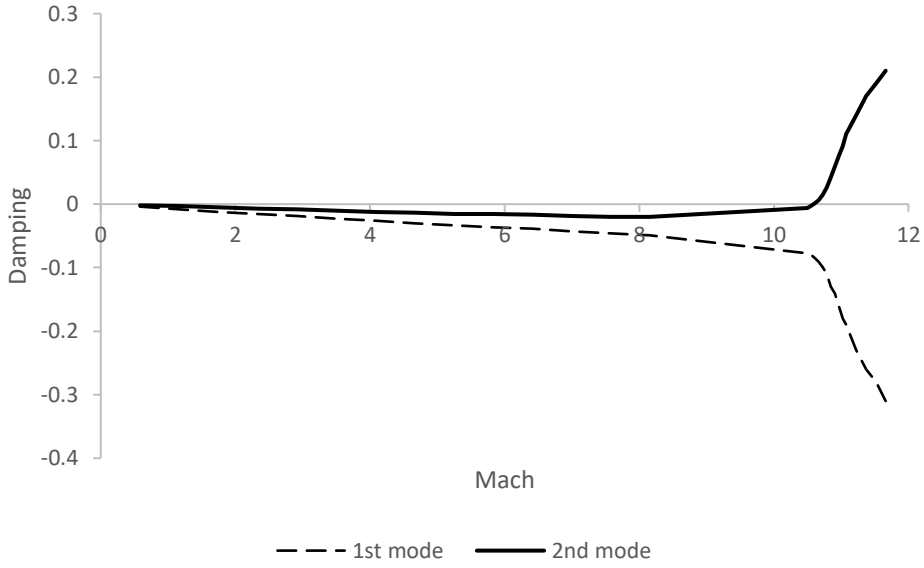

Figure 4. Damping-Mach graph of the supersonic fin with its brackets

Figure 4 shows the result of the aeroelastic analysis using a fin with its brackets. Flutter occurs at the critical condition when one of the modes' damping reaches zero (Hancock et al., 1985). As the flutter speed is approached, the frequencies of two normal modes converged (Niblett, 1988; Rheinfurth & Swift, 1966). Therefore, the results indicate an onset flutter of Mach 11 on the unbracketed fin and Mach 10.6 on the bracketed fin. The slightly lower flutter speed on the bracketed fin could be due to the more loose constraints applied on the bolt hole. In this configuration, the lateral motion of the holes is governed solely by the modeled spring elements, whereas in the unbracketed fin, the corresponding degree of freedom is entirely constrained. The computational analysis of the bracketed fin resulted in a more conservative flutter speed. However, the necessity of using a sophisticated model is not very strong for future

flutter analyses since the result difference is marginal, and the computed flutter speed also significantly exceeds the safety requirement of Mach 3.99.

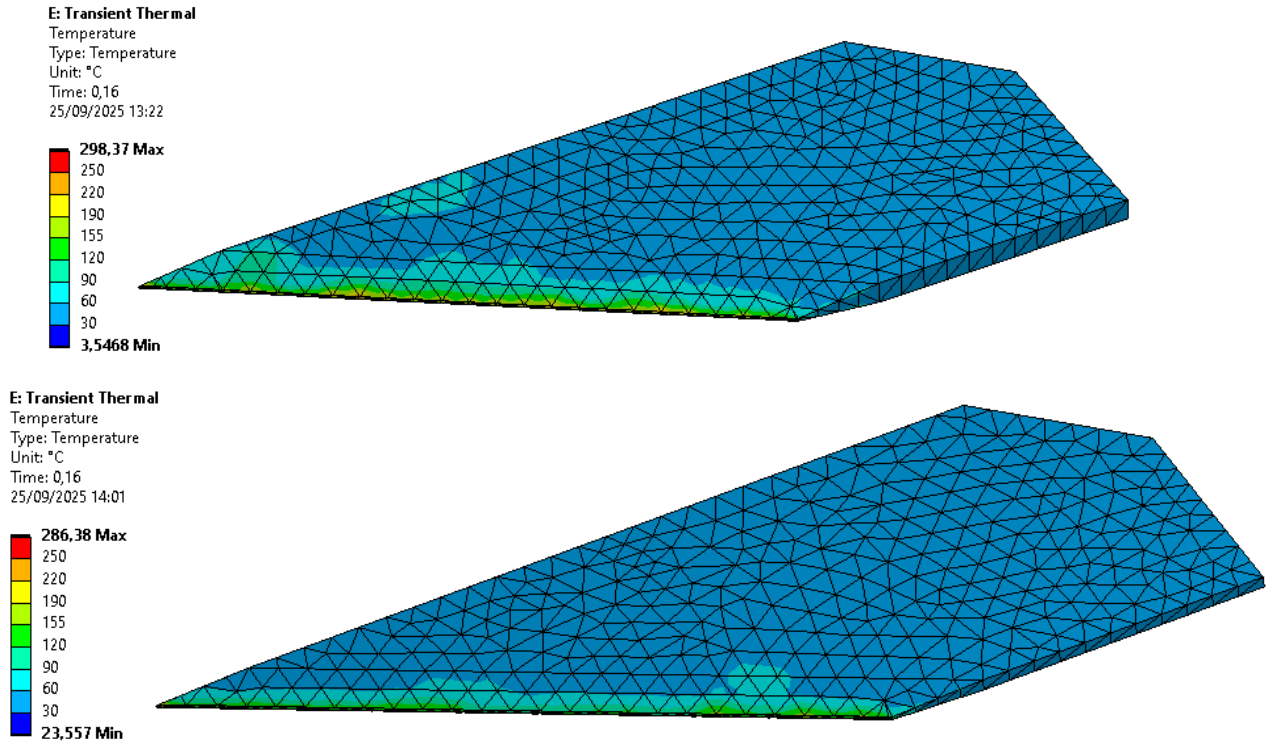

Figure 5. Temperature contour of a 25-mm-thick supersonic fin (above) and a 12-mm-thick supersonic fin (below) under thermal loading

Figure 5 demonstrates that the surface temperature of the fin with a thickness of 12 mm is generally lower than that of the fin with a thickness of 25 mm, where the region with surface temperature above 60 °C appeared wider. The larger aerodynamic heating of the 25-mm-thick fin compared to the 12-mm-thick fin is possibly due to the larger inclination angle of the former. The leading edge's inclination angle of the 25-mm-thick fin is 6.4°, and the leading edge's inclination angle of the 12-mm-thick fin is 2.6°. A shock wave can be established at an oblique orientation with respect to the supersonic flow (White, 1999). The temperature of the downstream could be greater than the temperature of the upstream (Wolff et al., 2024; Voklov, 2022; Khan et al., 2019). Using the following compressible flow equation for oblique waves as an approximation,

$$\frac{T_2}{T_1} = \left[1 + \frac{2\gamma}{\gamma+1}\left(M_1^2 \sin^2(\beta-\theta) - 1\right)\right]\frac{2 + (\gamma-1)M_1^2 \sin^2(\beta-\theta)}{(\gamma+1)M_1^2 \sin^2(\beta-\theta)}$$

where T_1 is the temperature before the shock wave, T_2 is the temperature behind the shock wave, γ is the ratio of specific heat capacities, M_1 is the Mach number before the shock wave, β is the shock wave angle, and θ is the structure's inclination angle, the inclination angle of the new fin design would result in a lower temperature behind the shock wave.

CONCLUSION

The combined aeroelastic and thermal evaluations of the redesigned supersonic fin with reduced thickness demonstrate its effectiveness in achieving both structural stability and enhanced thermal performance. Computational analyses on the aeroelasticity of the 12-mm fin resulted in a decrease of flutter speed from Mach 11.0 without brackets to Mach 10.6 with brackets. Both values substantially exceed the design requirement of Mach 3.99. This confirms that the inclusion of the fin brackets has only a marginal effect on flutter behavior and that the thinner fin design remains structurally stable under the considered operating conditions.

The lower aerodynamic heating experienced by the 12-mm-thick fin relative to the 25-mm-thick fin is possibly due to the lower inclination angle of its leading edge, which could generate a lower downstream temperature after a shock wave according to a supersonic flow equation. The analyses' results suggest that the new fin's geometry with a reduced thickness offers improved thermal performance in supersonic flow regimes.

Collectively, these outcomes support that the 12-mm supersonic fin not only satisfies aeroelastic stability requirements but also offers improved thermal behavior and significant mass efficiency. Nevertheless, future work should incorporate extended analyses under diverse structural loading conditions to fully establish the reliability and operational safety of the design.

REFERENCES

ANSYS, Inc. (2018). System Coupling User's Guide.

Bramsiepe, K., Voß, A., & Klimmek, T. (2020). Design and sizing of an aeroelastic composite model for a flying wing configuration with maneuver, gust, and landing loads. *CEAS Aeronautical Journal*, 11, 677-691.

Cavallo, T., Zappino, E., & Carrera, E. (2017). Component-wise vibration analysis of stiffened plates accounting for stiffener modes. *CEAS Aeronautical Journal*, 8, 385-412.

Cestino, E., Frulla, G., Spina, M., Catelani, D., & Linari, M. (2019). Numerical simulation and experimental validation of slender wings flutter behaviour. *Proceedings of the Institution of Mechanical Engineers, Part G: Journal of Aerospace Engineering*, 233(16).

Chen, F., Liu, H., & Zhang, S. (2018). Time-adaptive loosely coupled analysis on fluid–thermal–structural behaviors of hypersonic wing structures under sustained aeroheating. *Aerospace Science and Technology*, 78, 620-636.

Chen, G., Chen, W., Ji, L., Gao, T., & Lu, S. (2025). Trajectory-based flow-thermal-structural coupling analysis for hypersonic vehicles. *Physics of Fluids*, 37.

Chen, P.-C., & Liu, D.D. (1985). A Harmonic Gradient Method for Unsteady Supersonic Flow Calculations. *Journal of Aircraft*, 22.

Crotty, B. J. (1998). F-117A Accident during Air Show Flyover Caused by Omission of Fasteners in Wing-support Structure. *Flight Safety Foundation Aviation Mechanics Bulletin*, 46(5).

Ekadj, F. F., Nirbito, W., Hasim, F., Andika, M. G., Putro, I. E., & Mariani, L. (in press). Toward a Lightweight High-Speed Fin: Structural and Flutter Analysis for Thickness Reduction. *Aviation*.

Hancock, G. J., Wright, J. R., & Simpson, A. (1985). On the teaching of the principles of wing flexure-torsion flutter. *The Aeronautical Journal*, 89, 285-305.

Hexagon AB. (2021). MSC FlightLoads 2021.4 User's Guide.

Jones, W. P. (1948). Supersonic Theory for Oscillating Wings of Any Plan Form. *British Aeronautical Research Council R&M 2655*.

Ju, Q. & Qin, S. (2009). New Improved g Method for Flutter Solution. *Journal of Aircraft*, 46.

Khan, S. A, Aabid, A., Mokashi, I., Al-Robaian, A. A., & Alsagri, A. S. (2019). Optimization of Two-dimensional Wedge Flow Field at Supersonic Mach Number. *CFD Letters*, 11(5), 80-97.

Kuzenov, V. V., Ryzhkov, S. V., & Varaksin, A. Y. (2022). Calculation of Heat Transfer and Drag Coefficients for Aircraft Geometric Models. *Applied Sciences*, 12.

Martins, P. C. O., De Paula, A. S., Carneiro, S. H. S., & Rade, D. A. (2022). Hybrid control technique applied to an aero-servo-viscoelastic simplified wing model. *Aerospace Science and Technology*, 122.

Mazzoni, J. A., Filho, J. B. P., & Machado, H. A. (2005). Aerodynamic Heating on VSB-30 Sounding Rocket. *Proceedings of COBEM*.

Melhem, G. N., Bandyopadhyay, S., & Sorrell, C. C. (2014). Aerospace Fasteners in Mechanical and Structural Applications. *Annals of Materials Science & Engineering*, 1(4).

Niblett, L. T. (1988). A guide to classical flutter. *The Aeronautical Journal*, 92, 339-355.

Rheinfurth, M. H., & Swift, F. W. (1966). A New Approach to the Explanation of the Flutter Mechanism. *NASA-TN-D-3125*.

Rodden, W., Harder, R., & Bellinger, E. (1979). Aeroelastic Addition to NASTRAN. *NASA CR-3094*.

Salleh, Z., Hamid, A. H. A., Adnan, A. A., Muhammad, M. A., & Gwozdz, S. (2024). The Effects of Fin Cant Angle and Fin Height on the Performance of a Low Altitude Rocket. *International Journal of Integrated Engineering*, 16, 300-310.

Simmons, J., Deleon, A., Black, J., Swenson, E., & Sauter, L. (2009). Aeroelastic Analysis and Optimization of FalconLAUNCH Sounding Rocket Fins. *47th AIAA Aerospace Sciences Meeting including The New Horizons Forum and Aerospace Exposition*.

Syamsuar, S., Sampurno, B., Mahasti, K.M., Pratama, M.B.S., Sasongko, T.W., Kartika, N., Suksmono, A., Saputro, M.I.A., & Eskayudha, D.B. (2018). Half Wing N219 Aircraft Model Clean Configuration for Flutter Test On Low Speed Wind Tunnel. *Journal of Physics: Conference Series*, 1005(1).

Ujjin, R., Chaikiandee, S., & Ngaongam, C. (2021). Low Altitude Local Rocket Aerodynamics Analysis and Experimental Testing. *2nd Innovation Aviation & Aerospace Industry - International Conference*.

Ognjanović, O. V., Maksimović, S. M.,Vidanović, N. D., Šegan, S. D., & Kastratović, G. M. (2017). Numerical Aerodynamic-Thermal-Structural Analyses of Missile Fin Configuration During Supersonic Flight Conditions. Thermal Science, 21, 3037-3049.

Volkov, K. (2022). High-Temperature Effects on Supersonic Flow around a Wedge.

Wang, W., Qian, W., Bai, Y., & Wang, K. (2023). Numerical studies on the thermal-fluid-structure coupling analysis method of hypersonic flight vehicle. *Thermal Science and Engineering Progress*, 40.

Wemming, H., Lindström, S. B., Johansson, L., & Kapidžić, Z. (2023). Modelling and experimental parameter identification for fasteners in composite-aluminium bolted structures. *Composite Structures*, 323.

White, Frank M. (1999). Fluid mechanics. WCB McGraw-Hill.

Wolff, M., Abada, H.H., & Saad, H. A. K. (2024). Numerical Investigation of Supersonic Flow over a Wedge by Solving 2D Euler Equations Utilizing the Steger–Warming Flux Vector Splitting (FVS) Scheme.

Yang, Z., Li, J., Zhang, L., Tian, X., & Jiang, Y. Behaviors of Hypersonic Wing under Aerodynamic Heating. *Journal of Aerospace Engineering*, 34.

Zhiqiang, W., Nan, Y., Guoshu, L., & Chao, Y. Two-Way-Coupling Method for Rapid Aerothermoelastic Anlayses of Hypersonic Wings. *Transactions of Nanjing University of Aeronautics and Astronautics*, 35, 135-145.